

Rapid hydrothermal method for the preparation of carbon quantum dots in the presence of hydrogen peroxide

Jin-Lan Qin¹, Shan-Ji Li¹, Ning-Ning Yuan¹, Ying Chen¹, Bing-Fu Lei², Chao-Fan Hu² ✉, Ying-Liang Liu² ✉

¹School of petrochemical engineering, Guangzhou Institute of Technology, Guangzhou 510075, People's Republic of China

²Guangdong Provincial Engineering Technology Research Center for Optical Agriculture, College of Materials and Energy, South China Agricultural University, Guangzhou 510642, People's Republic of China

✉ E-mail: thucf@scau.edu.cn; tliuyl@scau.edu.cn

Published in Micro & Nano Letters; Received on 3rd September 2019; Revised on 8th March 2020; Accepted on 16th March 2020

Carbon quantum dots (CQDs) have been studied for years as one of the most promising fluorescent nanomaterials. Herein, CQDs were prepared rapidly by a simple, eco-friendly one-pot hydrothermal method in the presence of hydrogen peroxide. Different sizes of CQDs are obtained by changing the reaction time. X-ray photoelectron spectroscopy and Fourier transform infrared spectrometry demonstrated the existence of a large number of oxygen-containing groups on the surface of CQDs. The as-prepared CQDs exhibited bright yellow luminescence under UV light, they are applied for bioimaging of HeLa cells, and showed bright luminescence and excellent biocompatibility.

1. Introduction: In recent years, controllable synthesis of quantum dots (QDs) with various chemical elements have been developed, such as CdTe, CdSe [1] and ZnS [2]. They have excellent performance in fluorescence probes. However, most of the common synthesised QDs are containing cadmium or other heavy metals, and the high toxicity that caused may inhibit their bio-applications. Therefore, it is still necessary to develop other species of QDs with similar or better photoluminescence (PL) but higher biosafety. Carbon quantum dots (CQDs), tiny fluorescent particles, have drawn great attention as novel materials due to their excellent characteristics, such as unique luminescence, photostability, low toxicity, chemical resistance and electronic transport properties [3, 4]. In addition, CQDs can be prepared easily from a wide range of raw materials and they are particularly attractive due to their excellent bioimaging [5]. Therefore, CQDs have been proposed as promising substitutes for traditional QDs. The primary approaches for synthesising CQDs can be generally classified into two main groups: 'bottom-up' and 'top-down methods'. Bottom-up approaches refer to the synthesis of CQDs by assembling small molecular precursors (candles or gas soot, citrate salts, saccharides or carbohydrates), including solution chemistry [6], microwave-assisted method [7], ultrasonic-assisted method [8]. These methods are limited by severe synthetic conditions and time-consuming processes [9]. Top-down approaches refer to the cutting of some larger carbon structure, such as graphite, multiwalled carbon nanotubes into CQDs. Specific methods include alkali [10], chemical oxidation [11], electrochemical oxidation [12]. However, these methods may be limited because of their harsh reaction conditions, such as strong acid, strong base and strong oxidant. Therefore, it is still imminently needed to prepare high-quality CQDs by a simple, rapid and eco-friendly method.

Herein, we demonstrate a new method for extracting CQDs from commercially available AC by hydrothermal treatment in the presence of H₂O₂.

This method would show many advantages, including easily obtained carbon source, low cost, simple experimental performance and no need for additional strong acid or base. The synthetic CQDs have exhibited strong PL, excellent stability and solubility in water, as well as a narrow controllable particle size distribution. Furthermore, they are applied for bioimaging of HeLa cells, and showed bright luminescence and excellent biocompatibility. This work provides an efficient way for utilising AC as the raw material

to produce CQDs, which has never been reported before. It also can be applied to other materials, for example glucose, lignin and chitosan.

2. Experimental: CQDs are obtained by hydrothermal treatment of AC in the present of H₂O₂, 20 mg AC was mixed with 30 ml water in a glass vial by ultrasonic treatment of 5 min, the AC water dispersion was transferred to a Teflon lined autoclave and heated at 180°C for different time after mixed with 2 ml of ammonia solution (28 wt% in water). The reaction time range from 10 to 65 min, one every 5 min (we just take the representative samples in this paper). After cooling to room temperature, the unreacted activated carbon was filtered out using a mixed cellulose ester membrane with 0.22 µm Millipore. The filtrate was dialysed using 3500 Da dialysis membrane for 2 days to remove the H₂O₂, and the yellow powder of CQDs was obtained.

High-resolution transmission electron microscopy images were recorded using a JEOL-2010 electron microscope. Fourier transform infrared (FTIR) spectra were measured by an EQUINOX 55 (Bruker) spectrometer with the KBr pellet technique ranging from 500 to 4000 cm⁻¹. UV-Vis absorption spectra of the powder samples were performed using a Shimadzu UV-2550 ultraviolet-visible spectrophotometer. The X-ray diffraction (XRD) pattern was collected using a XD-2 ×/M4600. Nuclear magnetic resonance (NMR) spectra ¹³C of CQD samples dissolved in D₂O were recorded using a Bruker Avance 600 MHz spectrometer (Karlsruhe, Germany). The X-ray photoelectron spectroscopy (XPS) measurement was carried out on multi-functional photoelectron spectrometer. The fluorescence spectra of the CQDs were measured with a fluorescence spectrometer F-4500 (Hitachi, Japan).

Cell viability of CQDs was estimated by measuring the ability of cells to transform 3-(4,5-dimethyl-2-thiazolyl)-2,5-diphenyl-2-tetrazolium bromide (MTT) to a purple formazan dye. Cells were seeded in 96-well tissue culture plates at 2.0 × 10⁴ cells/well for 24 h. Next, the plates were incubated with different concentration of CQDs at 37°C in a 5% CO₂ atmosphere for 72 h, the medium was replaced by a solution of MTT, and then the cells were incubated with 20 µl per well of MTT solution (5 mg/ml⁻¹ in phosphate-buffered saline (PBS) for another 5 h. The reaction was terminated by adding 100 µl per well of dimethyl sulfoxide (DMSO) after removing the supernatant medium. When the purple formazan crystals were resolved by DMSO, the colour

intensity of the formazan solution reflects the cell growth condition, and were measured with a Bio-Rad ELISA reader at 570 nm.

Hela cells were seeded in each well of a confocal dish (Coverglass-Bottom Dish) and cultured at 37°C for 72 h. About 100 μ l of the CQDs were added into culture medium and incubated in regular cell culture conditions. After 2 h, medium with CQDs was removed from the cells and washed three times with 1 ml 1X PBS, and then the Hela cells were incubated with MitoTracker Red chloromethyl-X-rosamine (CMXRos) (50 nM) for 45 min and washed two times with 1 ml 1X PBS. Cellular uptake of CQDs by Hela cells was tracked via confocal microscopy under the excitation wavelength of 450, 490 and 633 nm, respectively.

3. Result and discussion: A facile one-step route to extract yellow luminescent CQDs from AC is demonstrated by a hydrothermal process, solely in the presence of H_2O_2 . As shown in Fig. 1, our method presents a relatively simple and low-cost method to produce CQDs without any strong acid or base. The synthetic process occurs in aqueous solution and has the advantage of being very cheap. H_2O_2 can be dissociated into hydroxyl radicals ($\cdot OH$) which has been considered as one of the most powerful oxidising species [13]. The prepared CQDs exhibit bright luminescence and excellent stability and solubility in water. The PL of the CQDs can be tailored by changing the reaction time. Namely, the size of CQDs can be edited just by controlling the reaction time, resulting in different PL of the CQDs (shallow – deep – shallow).

Fig. 2a shows a TEM image of CQDs with 20 min of hydrothermal treatments in the presence of H_2O_2 . The CQDs are of uniform spherical shape which was revealed to have a large distribution in the size range of 10–70 nm, the average size of CQDs was 30 nm (inset Fig. 2a). The CQDs with 50 min reacted time also were obtained (Fig. 2b), and the particles were also of uniform distribution but diameters were smaller than before, the size ranged from 1 to 4 nm with average size 2–3 nm (inset Fig. 2b). The result reveals that the reaction time can affect the size of CQDs and that longer reaction time leads to more smaller particles. This also can be demonstrated by Fig. S1. The HRTEM of CQDs with 50 min reacted time were investigated in Fig. 2c, in order to make it more clearly, we have magnified one of those lattice planes, it can be clearly identified with a spacing of 0.21 nm, which can be attributable to the (103) diffraction plan diamond-like (sp^3) carbon and the (102) lattice of graphitic (sp^2) carbon [14].

The XRD results for CQDs exhibit a (002) signal centred at around 25.8° (Fig. S2). A broad diffraction peak in the XRD pattern of CQDs may result from the small/thin nanostructures

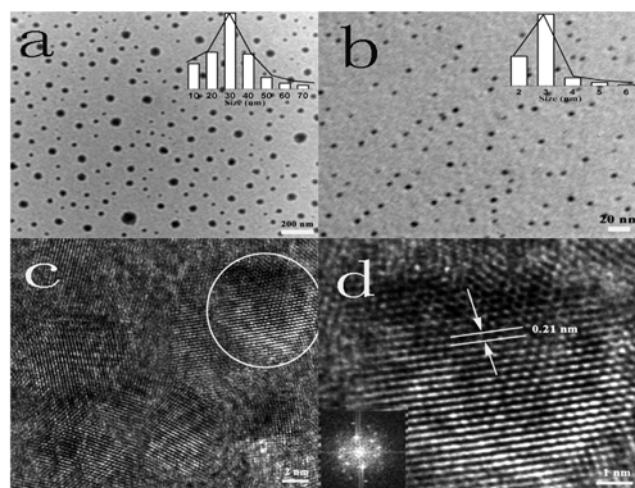


Fig. 2 TEM image and HRTEM images#
a, b TEM image and (inset) particle distribution of CQDs, corresponding to synthesised time with 20 and 50 min, respectively
c, d HRTEM image and inset corresponding to FFT analysis of CQDs

and weak layer–layer interactions [15]. From these analysis, it can be concluded that the hydrothermal method in the presence of H_2O_2 is a rapid and adjustable approach to prepare well-resolved lattice spacing of quantum-size materials.

To explore the chemical bonds and functional groups, FTIR spectrum of the AC (black line) and CQDs (red line) were also investigated in Fig. 3a, two strong wide peaks at 3386 and 3440 cm^{-1} are attributed to the presence of O–H, and the peaks at 1597 and 1621 cm^{-1} exhibit characteristic absorption bands of C=O, respectively.

Peaks at 1383 and 1389 are the characteristic absorption bands of C–OH, while the peaks at 1176 and 1069 correspond to the C–O stretching vibrations, respectively, and the peaks at 2922 and 2916 cm^{-1} can be ascribed to the absorption bands of C–H [16]. All analysis had demonstrated the existence of hydroxyl and carbonyl groups on the surface of AC and CQDs [17], and the FTIR spectrum of the CQDs shows stronger absorption bands of oxygen-related groups than AC, indicating the more oxygen-related groups on the surface of CQDs. UV–Vis spectra of CQD

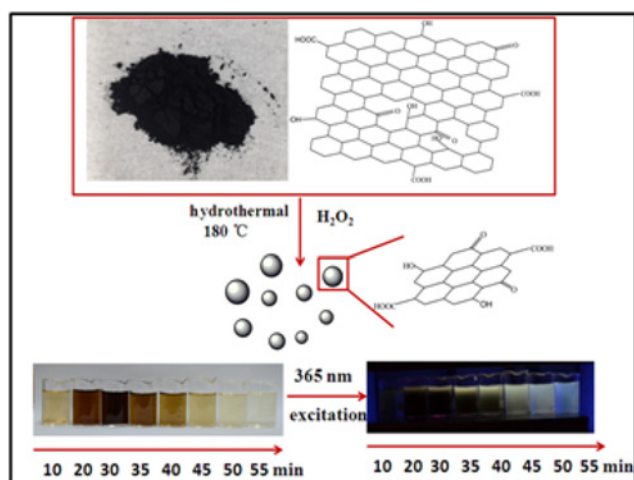


Fig. 1 Schematic illustration of the preparation of CQDs by hydrothermal treatment of AC in the presence of H_2O_2 and their luminescence

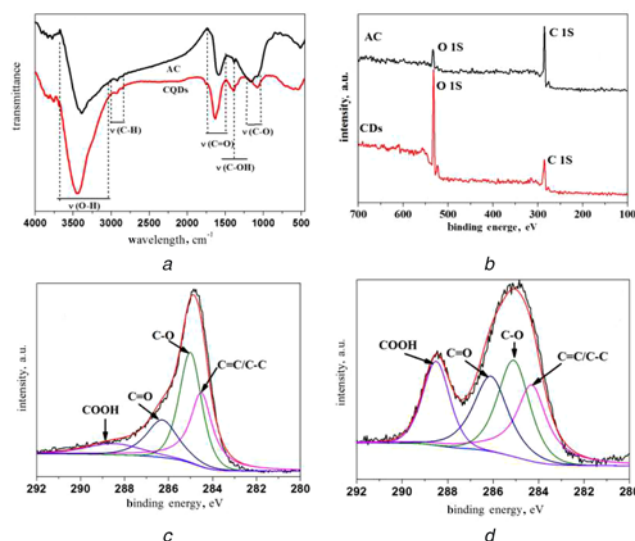


Fig. 3 FTIR spectra and XPS spectra
a FTIR spectra of AC and CQDs
b XPS spectra of AC and CQDs
c, d XPS C 1s spectra of AC and CQDs, respectively

are shown in Fig. S3, energy bandgap (E_g) can be calculated by the formula [18]

$$E = h(c/\lambda)$$

where E is energy bandgap, h is Planck's constant, c is speed of light and λ is a cut-off wavelength. Based on the UV-vis spectra of CQDs (Fig. S3), the cut-off wavelength is 323 nm, and the E_g is 0.384 eV. NMR spectra ^{13}C of CQD was employed to distinguish the types of hybridised carbon atom, as shown in Fig. S4, these signals in the range of 15–70 and 100–180 ppm were corresponding to both aliphatic carbon atoms (sp^3) and hybridised carbon atom (sp^2), respectively. The existence of carbon nuclei of carboxylic acid groups at the surface of CQD can be certified by the signals between 170 and 180 ppm [19, 20].

XPS measurements were carried out to probe the composition of AC (black line) and the CQDs (red line), as shown in Fig. 3b. AC peaks at 534 and 286 nm were attributed to the oxygen O1s and carbon C1s, respectively. The CQDs showed the existence of carbon (C1s, 284 eV), and oxygen (O1s, 532 eV) [21]. The C:O atomic ratios in AC and CQDs are 6.50 and 0.87, respectively, and the detailed data can be obtained in Table S1. The results from XPS spectra indicate that both AC and CQDs consist of carbon and oxygen but more oxygen-containing groups were existed in CQDs. The comparison of the high-resolution spectra of C1s peaks (Figs. 3c and d) demonstrates the obvious change in carbon chemical environment from AC to CQDs. This is provided by the observation of the following peaks: $\text{O}=\text{C}=\text{O}$, $\text{C}=\text{O}$, $\text{C}-\text{O}$ and $\text{C}=\text{C}$ function groups at 288.8, 286.3, 285.1 and 284.4 eV, respectively (Fig. 3c, AC of C1s) [20], and 288.5, 286.1, 285.1, 284.3 eV also can demonstrate the presence of $\text{O}=\text{C}=\text{O}$, $\text{C}=\text{O}$, $\text{C}-\text{O}$ and $\text{C}=\text{C}$ function group (Fig. 3d, CQDs of C1s), indicated CQDs were functionalised with hydroxyl, carbonyl and carboxylic acid groups and suitable for luminescence emission.

As we expected, the CQDs can present bright emission under the ultraviolet radiation (365 nm), as shown in Fig. 1, the PL and excitation spectra of CQDs with synthesised time of 10, 20, 30, 35, 40, 45, 50 and 55 min, were investigated in Figs. 4a and b, respectively. In order to study the luminescence of CQDs with

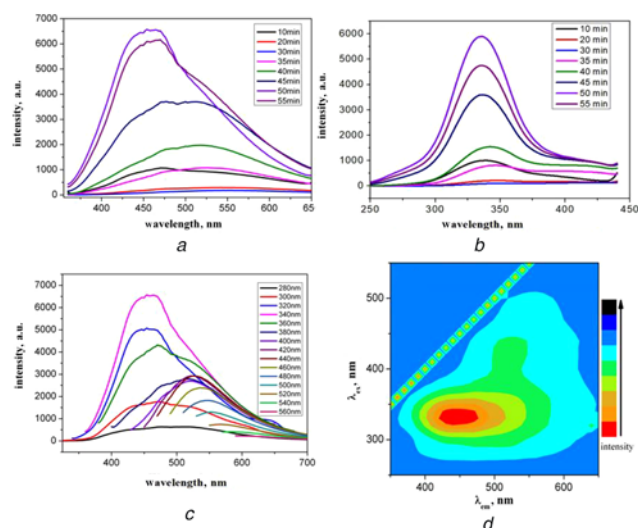


Fig. 4 Optical properties of CQDs

a Excitation spectra of CQDs with different synthesised time

b Intensity of corresponding PL peak

c Excitation-dependent fluorescence emission of CQDs with 50 min synthesised time

d Different emission contour plot and different excitation corresponding to synthesised time

50 min hydrothermal time more clearly, Fig. 4c shows their peaks of emission red-shift depend on the excitation, and when excitation is 340 nm, the emission reach maximum and peaks located at 450 nm, and these result correspond with that of the reported [22]. Fig. 4d refers to different emission contour plot different excitation of CQDs with 50 min synthesised time, the red colour presents the energy is the highest, and then the orange, the black is lowest. From the vivid and clear picture we can know that the optimal excitation is about 340 nm, and the peak is located at 450 nm. In addition, the emission peak shows a slightly red shift with the increase in pH value, as shown in Fig. S5. All those results indicate that the CQDs are suitable materials for bioimaging.

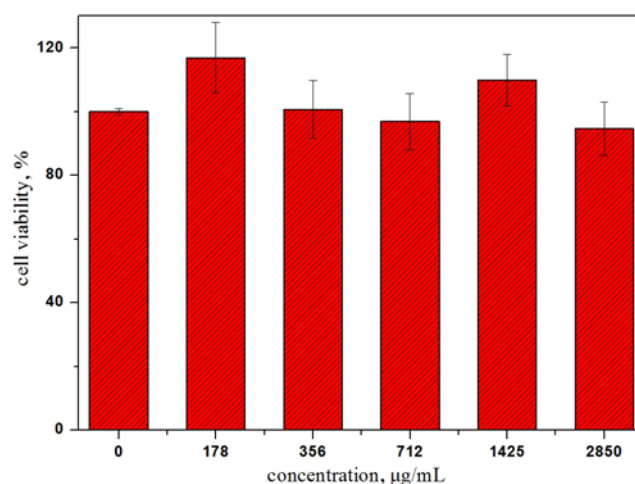


Fig. 5 Cell viability of HeLa cells incubated with different concentration of CQDs

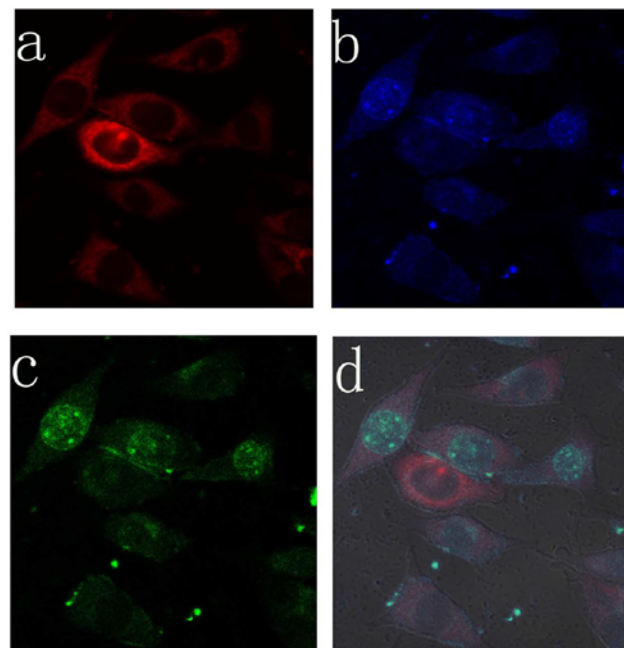


Fig. 6 Confocal fluorescence microphotograph of HeLa cell incubated with CQDs

a, b, c Confocal fluorescence microphotograph of HeLa cell after incubation with CQDs under 633, 450, 490 nm excitation

d Overlay of high contrast image of HeLa cell stained with red CMXRs and CQDs (blue, green) staining

As reported [5, 23], the CQDs can be used for biological application such as bioimaging, cancer diagnostic probe, gene technology, among those application, the inherent toxicity of the materials must be within limits, therefore, the cytotoxicity of CQDs was evaluated by carrying out a series of MTT assays using the HeLa cells. As observed in Fig. 5, none of the HeLa cell lines show any statistically significant difference in cell survival after 72 h, even the concentration ranged from 178 to 2850 µg/ml. The MTT assays of cell viability studies suggested that the CQDs do not impose a considerable toxicity to HeLa cells compared to the control.

It has reported that the CQDs can be used as cellular imaging [17], in order to determine that, we chose MitoTracker Red CMXRos (50 nM), a commercially available mitochondrial fluorescent probe to show red colour under imaging [18], as shown in Fig. 6a, the obtained images clearly visualise the phase image of HeLa cells, major mitochondria stained red with CMXRos under 633 nm excitation.

Furthermore, agglomerated high fluorescent image of CQDs exhibits blue and green around each nucleus under 450 and 490 nm excitation (Figs. 6b and c). Fig. 6d is the high overlay contrast image of nucleolus stained with blue, green and red CMXRos staining. Intriguingly, the nucleus of HeLa can be precisely targeted by CQDs, which indicate that the CQDs can be used in high contrast bioimaging and other biomedical applications.

4. Conclusion: Luminescent CQDs were synthesised by one-pot hydrothermal treatment in the presence of hydrogen peroxide. Different size of CQDs has been synthesised by changing the reaction time. FTIR, XPS spectra have confirmed the synthetic CQDs have a large of oxygen-containing groups on the surface, and the CQDs show good luminescence and water solubility. This simple, eco-friendly and cheap process represent a potential advancement for controllable size production. Coupled with low cytotoxicity, the CQDs provide promising application for bioimaging and biosensing applications.

5. Acknowledgments: The present work was supported by the National Natural Science Foundations of China (grant nos. 21571067, 21671070) Innovation Team Project in Universities of Guangdong Province (Natural Science) (grant no. 2017GKCXTD006).

6 References

- [1] Zhang Z.P.: 'Graphene quantum dots: an emerging material for energy-related applications and beyond', *Energy Environ. Sci.*, 2012, **5**, pp. 8869–8890
- [2] Al-Douri Y.: 'Optical investigations of blue shift in ZnS quantum dots', *Superlattices Microstruct.*, 2015, **88**, pp. 662–667

- [3] Tang J.Z.: 'Carbon dots as an additive for improving performance in water-based lubricants for amorphous carbon (a-C) coatings', *Carbon.*, 2020, **156**, pp. 272–281
- [4] Ma Y.J.: 'Preparation and characterisation of multifunctional magnetic-fluorescent Fe₃O₄/carbon dots/silica composites', *Micro Nano Lett.*, 2013, **8**, pp. 302–304
- [5] Hu Y.F.: 'Biomass-codoped carbon dots: efficient fluorescent probes for isocarbophos ultrasensitive detection and for living cells dual-color imaging', *J. Mater. Sci.*, 2019, **54**, pp. 8627–8639
- [6] Mueller M.L.: 'Triplet states and electronic relaxation in photoexcited graphene quantum dots', *Nano Lett.*, 2010, **10**, pp. 2679–2682
- [7] Yang P.: 'Microwave-assisted synthesis of xylan-derived carbon quantum dots for tetracycline sensing', *Opt. Mater.*, 2018, **85**, pp. 329–336
- [8] Zhou S.J.: 'Upconversion and downconversion fluorescent graphene quantum dots: ultrasonic preparation and photocatalysis', *ACS Nano.*, 2012, **6**, pp. 1059–1064
- [9] Li H.T.: 'Carbon nanodots: synthesis, properties and applications', *J. Mater. Chem.*, 2012, **22**, pp. 24230–24253
- [10] Li W.: 'Preparation of the alkaline lignin pyrolytic based carbon quantum dots/TiO₂ composite photocatalyst', *J. For. Eng.*, 2016, **1**, pp. 84–88
- [11] Dong Y.Q.: 'One-pot and high yield simultaneous preparation of single- and multi-layer graphene quantum dots from CX-72 carbon black', *J. Mater. Chem.*, 2012, **22**, pp. 8764–8766
- [12] Li Y.: 'An electrochemical avenue to green-luminescent graphene quantum dots as potential electron-acceptors for photovoltaics', *Adv. Mater.*, 2011, **23**, pp. 776–780
- [13] Zhou X.J.: 'Photo-Fenton reaction of graphene oxide: a new strategy to prepare graphene quantum dots for DNA cleavage', *ACS Nano*, 2012, **6**, pp. 6592–6599
- [14] Lei T.: 'Nanosized carbon particles from natural gas soot', *Chem. Mater.*, 2009, **21**, pp. 2803–2809
- [15] Zhan Y.: 'Near-ultraviolet to near-infrared fluorescent nitrogen-doped carbon dots with two-photon and piezochromic luminescence', *ACS Appl. Mater. Interfaces.*, 2018, **10**, pp. 27920–27927
- [16] Gao M.X.: 'A surfactant-assisted redox hydrothermal route to prepare highly photoluminescent carbon quantum dots with aggregation-induced emission enhancement properties', *Chem. Commun.*, 2013, **49**, pp. 8015–8017
- [17] Huang C.X.: 'Synthesis of carbon quantum dot nanoparticles derived from byproducts in bio-refinery process for cell imaging and in vivo bioimaging', *Nanomaterials*, 2019, **9**, pp. 387–397
- [18] Al-Douri Y.: 'Synthesis of carbon-based quantum dots from starch extracts: optical investigations', *Luminescence*, 2018, **33**, pp. 260–266
- [19] Dou Q.: 'Multi-functional fluorescent carbon dots with antibacterial and gene delivery properties', *RSC Adv.*, 2015, **5**, pp. 46817–46822
- [20] Ding Z.: 'Gram-scale synthesis of single-crystalline graphene quantum dots derived from lignin biomass', *Green Chem.*, 2018, **20**, pp. 1383–1390
- [21] Shen R.: 'Raman fluorescence enhancement of bare carbon dots through facile reduce chemistry', *Chem. Phys. Chem.*, 2012, **13**, pp. 3549–3555
- [22] Hessel C.M.: 'Cooper selenide nanocrystals for photothermal therapy', *Nano Lett.*, 2011, **11**, pp. 2560–2566
- [23] Molkenova A.: 'Rapid synthesis of nontoxic and photostable carbon nanoparticles for bioimaging applications', *Mater. Lett.*, 2020, **261**, p. 127012